Journal of Hydroscience and Hydraulic Engineering
Vol. 7, No. 1, November, 1989, pp.35-49

OSCILLATORY FLOW FORCES ON CYLINDERS PLACED ON THE BOTTOM BOUNDARY

By

Syunsuke Ikeda

Prof., Dept. of Foundation Engrg., Saitama Univ., Urawa, Saitama, Japan

and

Yoshimichi Yamamoto

Research Engr., INA Shin-Doboku Kenkyusho, Tokyo, Japan

SYNOPSIS

The forces acting on circular cylinders placed on plane boundary are studied in a sinusoidally oscillating flow generated in a U-shaped water tunnel. The resultant force is divided in three parts, i.e. inertia, drag and lift forces. The inertia coefficients are found to be significantly correlated with the KC number and a weak function of flow acceleration. The drag coefficients show essentially a unique function of KC number for KC > 7. They decrease as the KC number increases, and finally take a constant value of 1.2. The lift coefficients are well correlated with the KC number and flow acceleration. The lift force is mainly produced by mean velocity field, and vortices play a minor role. The trace of lift force with time is fairly stable compared with that of the cylinder immersed in oscillating flow of large extent. Flow visualization reveals that the separation point is closely correlated with the flow acceleration, which explains the reason why the inertia and lift coefficients are grouped by the flow acceleration.

INTRODUCTION

For a rational design of circular pipes and cables placed on sea bottom, forces acting on them have become a subject of investigation in recent years. The subject includes several complicated phenomena such as separation of flow, vortex shedding and decaying, turbulence, unsteadiness of flow, proximity effect, and therefore the subject still requires further research.

Nagasaki and Ogata (5) measured wave induced added mass, drag and lift coefficients of circular pipes placed on a plane boundary, and they correlated the coefficients with depth/wavelength ratio and waveheight/wavelength ratio. Yamamoto, et al. (8) evaluated the forces with potential flow theory, and found that the theory explains the actual fairly well as far as the vortex force is negligible. Sarpkaya (6,7) studied the proximity effect on inertia, drag and lift coefficients of circular cylinders submerged in sinusoidally oscillating flows generated in a U-shaped water tunnel. He found that these coefficients are well correlated with the KC number which Keulegan and Carpenter (2) proposed and gap/cylinder diameter ratio. It was found that the lift force is comparable with the drag force. Wright and Yamamoto (9) found that lift force is large compared with the other forces and directs from the plane boundary for circular cylinders placed on the boundary.

These works shed light on the subject to considerable extent, and yet accumulation of the data is not sufficient, and little is known on the cause and the internal structure of the coefficients.

The present work was performed in a water tunnel described in a separate

paper (see Ref. 1). The inertia, drag and lift coefficients were measured in detail for circular cylinders placed on the plane boundary. Flow separation and vortex shedding were observed using polystyrene particles, and the flow visualization made it possible to explain how these forces were generated. These cofficients were found to be significantly correlated with the KC number and a new parameter describing the acceleration of oscillatory flow.

FORCE COEFFICIENTS

Morison, et al. (4) assumed the in-line force to consist of the inertia force F_M and the drag force F_D, and it is described by

$$F_X = F_M + F_D = \rho C_M \frac{dU}{dt} \frac{\pi}{4} D^2 + \frac{1}{2} \rho C_D U|U| D \qquad (1)$$

in which F_X = in-line force acting on a circular cylinder of diameter D per unit length, ρ= mass density of fluid, C_M = inertia coefficient, C_D = drag coefficient, U = undisturbed oscillatory flow velocity, and t = time.

Keulengan and Carpenter (2) defined the Fourier averages of C_M and C_D as follows:

$$C_M = \frac{2}{\pi^2} \frac{U_m T}{D} \int_0^{2\pi} \frac{F_X \sin\omega t}{\rho U_m{}^2 D} d(\omega t) \qquad (2)$$

$$C_D = -\frac{3}{4} \int_0^{2\pi} \frac{F_X \cos\omega t}{\rho U_m{}^2 D} d(\omega t) \qquad (3)$$

in which ω = angular frequency of undisturbed oscillating flow ($2\pi/T$), U_m = half-amplitude of undisturbed fluid velocity, and T = period of oscillating flow.

For cylinders immersed in an oscillatory flow of large extent, the frequency of the lift force varies according to that of vortex shedding even if the period of oscillatory flow is idential, and the same definition as the inertia and drag coefficients cannot be applied to the lift coefficient (see Refs. 1 and 7). It is defined by

$$F_L = \frac{1}{2} \rho C_L U_m{}^2 D \qquad (3)$$

in which F_L = maximum lift force per unit length in a cycle of oscillatory flow, and C_L =lift coefficient. F_L fluctuates considerably for each cycle of the oscillatory flow and lift force is much larger than the other forces as mentioned subsequently, and the knowledge on the possible maximum lift force is required from the practical point of view. Thus, the following significant lift coefficient is introduced:

$$\overline{C}_{L\,max} = \frac{(\text{average of the one-tenth largest } F_L)}{\frac{1}{2} \rho U_m{}^2 D} \qquad (5)$$

DIMENSIONAL ANALYSIS

For the characteristic fluid forces (such as the maximum force) on elastically mounted circular cylinders immersed in sinusoidally oscillating flows generated in a U-shaped water tunnel, the associated parameters are diameter of cylinder D, half-amplitude of undisturbed fluid velocity U_m, density of fluid ρ, fluid viscosity μ, period of oscillating flow T, gravity g, and natural frequency of the elastically mounted cylinder f_n. The forces on cylinder per unit length F should be expressed by

$$F = \Psi(D, U_m, \rho, \mu, T, g, f_n) \tag{6}$$

in which Ψ = function. The dimensionless, independent variables should be five, and the suitable choice is

$$\frac{F}{\rho U_m^2 D} = \Psi\left(\frac{U_m T}{D}, \frac{U_m}{gT}, \frac{\sqrt{\nu T}}{D}, f_n T\right) \tag{7}$$

or

$$\frac{F}{\rho D^2 \frac{U_m}{T}} = \phi\left(\frac{U_m T}{D}, \frac{U_m}{gT}, \frac{\sqrt{\nu T}}{D}, f_n T\right) \tag{8}$$

in which ν = kinematic viscosity of fluid, $U_m T/D$ = KC number, and Ψ and ϕ = functions. The Reynolds number is known to have negligible effect on the force coefficients of circular cylinders in the oscillating flow with the Reynolds number below 2×10^5, and it is not used as a meaningful parameter (see e. g. Ref. 2). The parameter $U_m T/D$ is interpreted to be a dimensionless fluid particle amplitude of undisturbed flow. U_m/gT is the bulk acceleration of undisturbed flow. $\sqrt{\nu T}/D$ is the boundary layer thickness/cylinder diameter ratio and also a measure of dissipation of vortices shed into flow field around the cylinder (see Ref. 1). $f_n T$ may be insignificant if the natural frequency is much larger than the vortex shedding frequency.

If U_m^2 is displaced by $U|U|/2$ and F is regarded as F_D in the right of Eq. 7, the right hand side reduces to the definition of drag coefficient, and if F is replaced by $2F_L$, it becomes the lift coefficient. Similarly, Eq. 8 is interpreted to be the inertia coefficient if F and U_m/T are displaced by F_M and $(\pi/4)dU/dt$, respectively.

Thus, the force coefficients are expected to correlate with $U_m T/D$, U_m/gT and $\sqrt{\nu T}/D$.

EXPERIMENTAL APPARATUS AND PROCEDURE

A U-shaped water tunnel is used to yield sinusoidally oscillating flow. The water tunnel is 14m long with a straight working reach of 6.2m long. The working reach is made of plexiglass, and its cross section is 30 by 30 cm. The water is moved by a piston driven by a DC motor. The maximum half-amplitude of the oscillating flow is 35 cm, and the period is variable from 1 to 20 sec. The oscillating flow is monitored with a hotfilm anemometer, and it is found that sinusoidal oscillating flow is well established.

Three kinds of circular cylinders made of plexiglass were used to measure the in-line and lift forces. The physical properties of the cylinders are shown in Table 1. The cylinders were placed horizontally at a working section located at about the middle of the working reach. The length of each cylinder

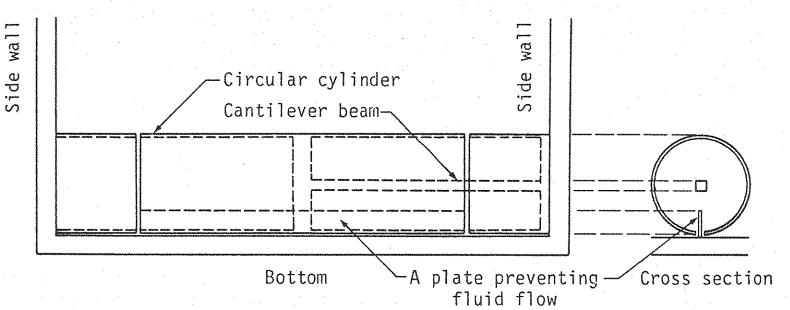

Fig. 1. Circular Cylinder for Measurement of Forces.

is made shorter than the width of the channel to exclude the side wall effect, and the shortage parts are replaced by two cylinders attached rigidly to the walls. At the bottom of each cylinder, a slit spanned the total length of the cylinder is opened, and a thin plate which is fixed to the channel floor is inserted in the slit. This device was prepared to prevent water from flowing through small gap between the cylinder and the floor (see Fig. 1)

The force measuring device is composed of strain-gaged cantilever beam mounted rigidly to one side wall, and another end of the beam is tightly attached to an appropriate part of the cylinder. The output of the strain-gages were calibrated using a spring balance with an accuracy of 1 gr (= 980 dyn), and the calibration was performed by hanging weight.

The analogue signals of the hotfilm anemometer and the strain-gages are onlined to a digital computer through an interface. The force measuring experiments were conducted under two constraints. One is that the natural frequency of submerged cylinder should be more than ten times larger than that of the vortex shedding in order to avoid resonance. Another constraint is that the strain of the gages is larger than 10^{-5} to keep accuracy. The forces were measured for sequential 50 cycles of oscillatory flow.

The flow field around cylinders is visualized with fine polystyrene particles with a median diameter of 0.45mm and a specific gravity of 1.04. Shedding a slit ray through the above transparent wall, the motion of the particles was recorded with a 16mm cinecamera. The motion pictures were taken at a rate of 12 frames per sec, and they were used to determine the flow separation point and to trace the movement of vortices produced around cylinders.

RESULTS

The inertia and drag coefficients evaluated using Eqs. 2 and 3 showed a little unsteadiness for each cycle of the oscillatory flow, though the fluctuation was small. To exclude the unsteadiness, the coefficients are ensemble averaged over 50 cycles of oscillatory flow, and they are expressed by

$$\overline{C}_M = \frac{\sum_{i=1}^{50} C_{Mi}}{50} \tag{9}$$

$$\overline{C}_D = \frac{\sum_{i=1}^{50} C_{Di}}{50} \tag{10}$$

in which the subscript i = number of sequential cycle of oscillatory flow.

The fluctuation was also found for the lift coefficient, though it is small compared with that found for cylinders immersed in oscillatory flow with large extent for which the cause of fluctuation is due to instability of vortex shedding (see Ref. 1). Thus, the same procedure as Eqs. 9 and 10 is applid to the lift coefficient. It is defined by

$$\overline{C}_L = \frac{\sum_{i=1}^{50} C_{Li}}{50} \tag{11}$$

The averaged inertia coefficients $\overline{C}_M$ are depicted in Fig. 2 as a function of $KC = U_m T/D$ and a_m/g, in which a_m = half-amplitude of acceleration of undisturbed oscillating flow. For sinusoidal displacement of undisturbed fluid particle, $x = A\sin 2\pi t/T$, in which x = location of fluid particle at time t and A = half-amplitude, the acceleration of fluid is

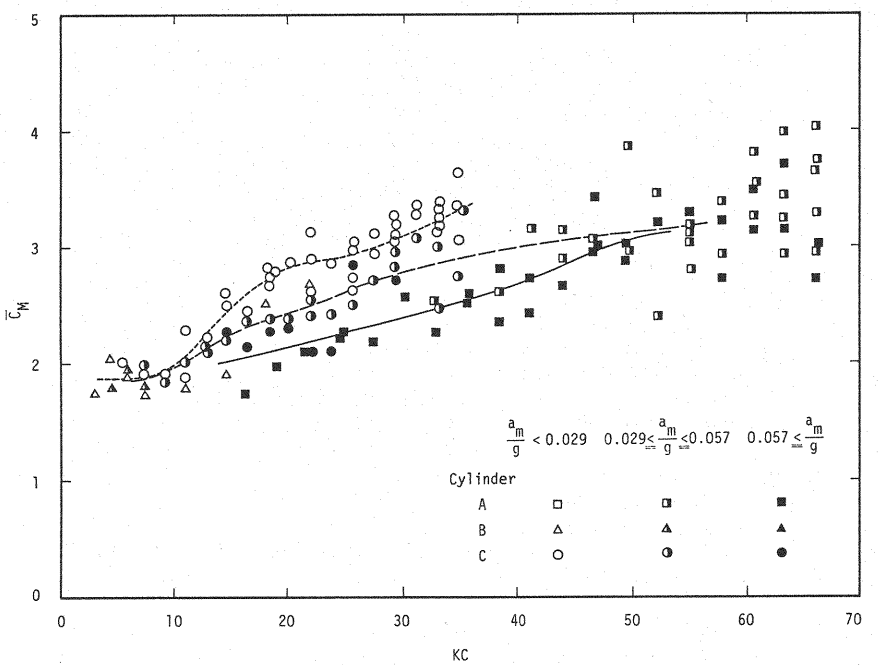

Fig. 2. Inertia Coefficient.

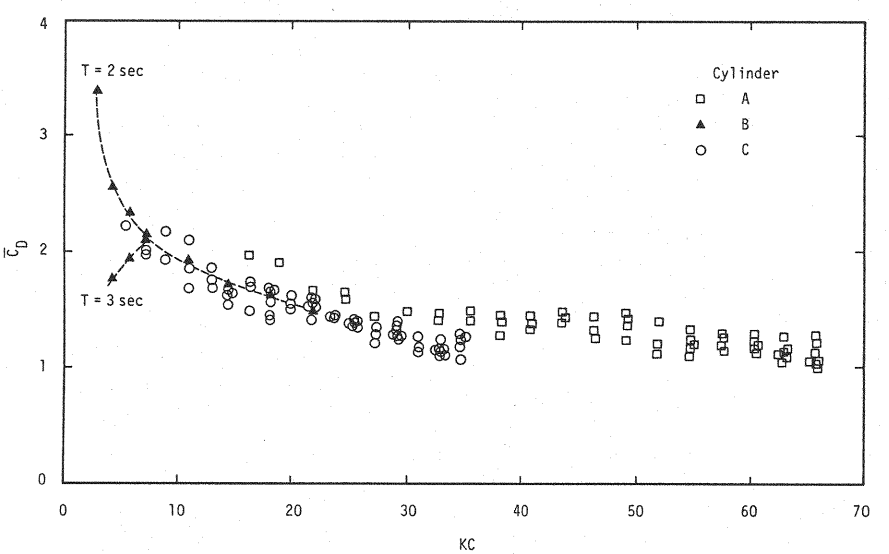

Fig. 3. Drag Coefficient.

$$\frac{dU}{dt} = - (2\pi)^2 \frac{A}{T^2} \sin \frac{2\pi t}{T} \qquad (12)$$

From which $a_m = (2\pi)^2 A/T^2 = 2\pi U_m/T$ or $(2\pi KC)D/T^2$ $(KC = 2\pi A/D)$. At low KC numbers smaller than about 10, the coefficients take an essentially constant value of 1.8 which is a little smaller than that of potential flow with large extent, for which the inertia coefficient is calculated to be 2. As the KC number increases, they have a trend to increase monotonously, and the scatters also increase. The scatters can be grouped reasonably if they are parameterized by a_m/g $(= 2\pi U_m/gT)$. The reason will be described later based on flow visualization. For cylinders immersed in the oscillatory flow of large extent, it is reported that the inertia coefficients have a minimum value of 0.75 at about KC = 12, and they increase gradually to reach 2.5 for KC > 100 (see Ref. 2). The reason of the discrepancy between the two situations may be sought in the existence of the bottom boundary.

The drag coefficients $\overline{C}_D$ are plotted against the KC number in Fig. 3, and they show less scatters than the inertia coefficients. They can be regarded as a single line for KC > 7, and they decrease gradually with increasing the KC number. The coefficients finally reach a constant value of about 1.2 for sufficiently large KC numbers, and the value is identical with that for unidirectional flow. The drag coefficients measured in the present study are nearly identical with the values observed by Keulegan and Carpenter (2) for KC > 20. However, they reported a remarkable peak in the vicinity of KC = 10, which could not be found clearly in the present work. The drag coefficients in Fig. 3 show multivalues for KC < 7 even if the identical cylinder (D = 6 cm, f_n = 18.5 Hz) and measuring device are used. As the KC number decreases, the lower branch (T = 3 sec) takes a peak at KC = 7 and then decreases. The upper branch (T = 2

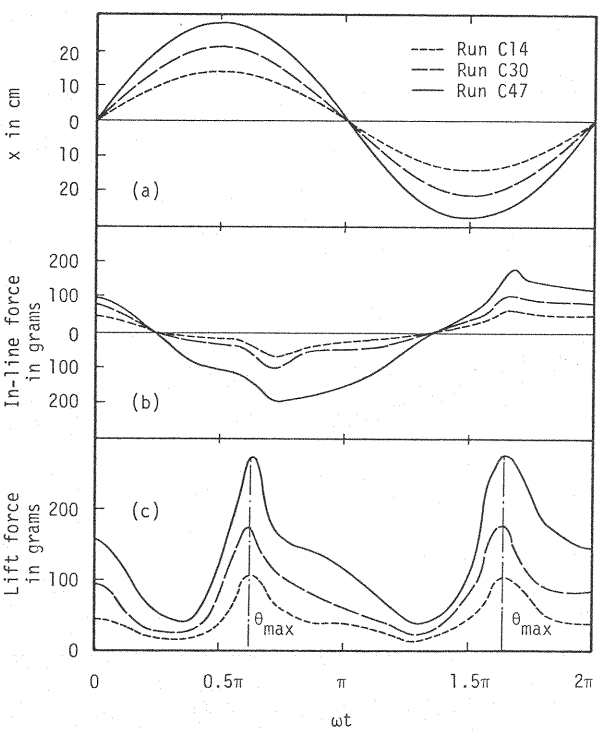

Fig. 4. Time Variation of (a) Location of Undisturbed Particle; (b) In-line Force; and (c) Lift Force.

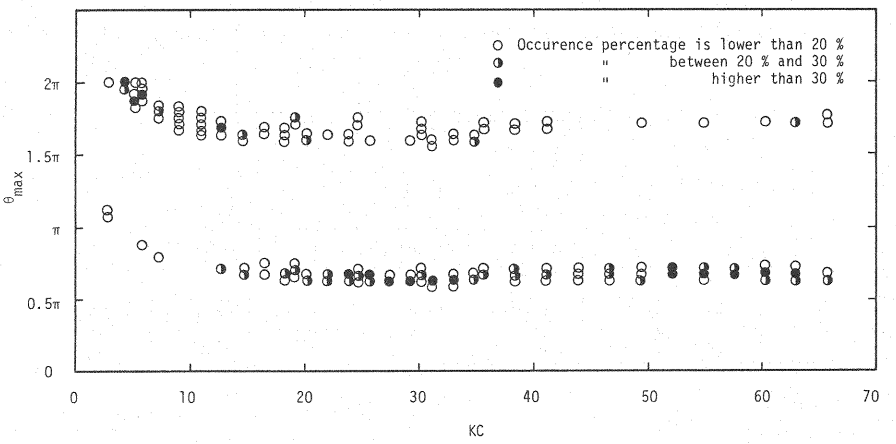

Fig. 5. Phase at which the Maximum Lift Force Occurs.

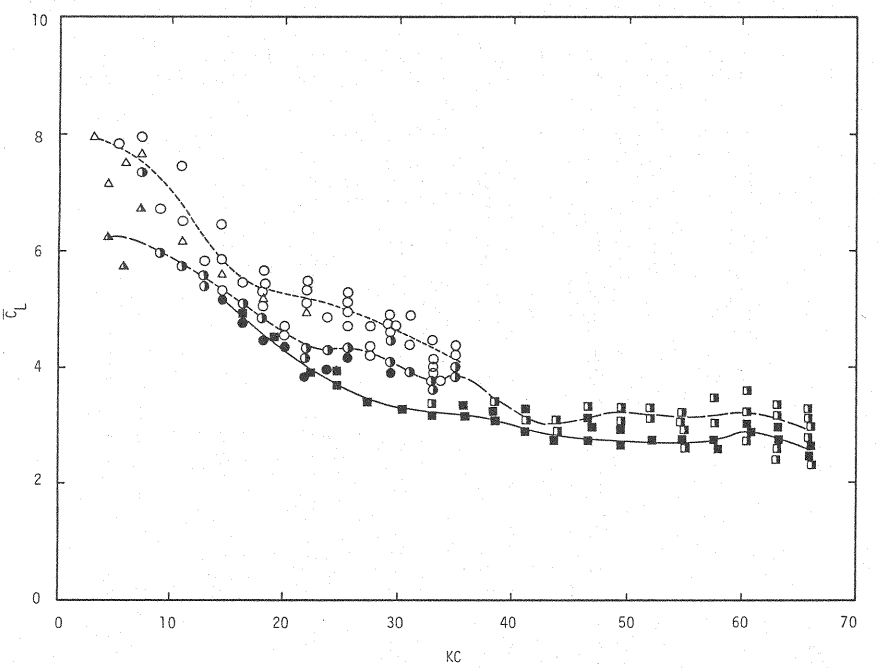

Fig. 6. Lift Coefficient. Symbols are as in Fig. 2.

sec), however, monotonously increases as the KC number decreases. Thus, the coefficients seem to depend not only on the KC number but also on the period of oscillatory flow (or the acceleration of flow). The definite conclusion, however, requires more data.

The time trace of lift force seems to have a similar pattern regardless of the KC number if the time scale is normalized by the period of oscillatory flow,

Table 1. Cylinders used. It should be noted that 1 gram = 980 dyn.

Circular cylinder	Diameter in centimeters	Weight of circular cylinder in grams	Natural frequency in water in Hertz		Cross section of cantilever in millimeters
			Horizontal	Vertical	
A	3.2	105	43.9	47.1	10.9×10.9
B	6.0	190	16.0	18.5	10.1×10.1
C	6.0	195	23.8	25.5	10.9×10.9

Table 2. Force Coefficients for Cylinder A.

Run	A, in centi-meters	T, in seconds	KC number	Acceler-ation of flow, a_m/g	Inertia coeffi-cient, $\overline{C}_M$	Drag coeffi-cient, $\overline{C}_D$	Lift coeffi-cient $\overline{C}_L$	Significant lift coefficient $\overline{C}_{Lmax}$
A1	8.4	2.0	16.5	8.46×10^{-2}	1.72	1.99	4.93	5.73
A2	9.8	2.0	19.2	9.87	1.98	1.92	4.51	4.95
A3	11.2	2.5	22.0	7.22	2.09	1.67	3.79	4.64
A4	12.6	2.5	24.7	8.12	2.28	1.65	3.66	4.41
A5	12.6	2.5	24.7	8.12	2.24	1.64	3.93	4.56
A6	14.0	3.0	27.5	7.27	2.17	1.45	3.37	3.87
A7	15.4	3.0	30.2	6.89	2.58	1.48	3.26	3.69
A8	16.8	3.0	33.0	7.52	2.25	1.48	3.15	3.68
A9	16.8	3.5	33.0	5.52	2.49	1.47	3.33	3.91
A10	18.2	3.0	35.7	8.15	2.52	1.48	3.20	3.72
A11	18.2	3.5	35.7	5.99	2.59	1.40	3.24	4.03
A12	19.5	3.0	38.3	8.73	2.35	1.42	3.11	3.48
A13	19.5	3.5	38.3	6.41	2.82	1.44	3.23	3.81
A14	19.5	4.0	38.3	4.91	2.62	1.29	3.34	4.00
A15	20.9	3.0	41.0	9.35	2.42	1.45	2.88	3.36
A16	20.9	3.5	41.0	6.87	2.73	1.39	3.23	3.74
A17	20.9	4.0	41.0	5.26	3.15	1.37	3.06	3.72
A18	22.3	3.5	43.8	7.33	2.65	1.44	2.75	3.09
A19	22.3	4.0	43.8	5.61	3.14	1.43	3.03	3.42
A20	22.3	4.5	43.8	4.44	2.90	1.47	2.83	3.50
A21	23.7	3.5	46.5	7.79	2.94	1.26	3.05	3.57
A22	23.7	4.0	46.5	5.97	2.98	1.32	2.70	3.14
A23	23.7	4.0	46.5	5.97	3.42	1.44	3.05	3.69
A24	23.7	4.5	46.5	4.71	2.99	1.31	3.31	4.10
A25	25.1	3.5	49.3	8.25	2.88	1.41	2.90	3.31
A26	25.1	4.0	49.3	6.32	3.00	1.23	2.63	3.03
A27	25.1	4.5	49.3	4.99	2.94	1.41	2.97	3.42
A28	25.1	5.0	49.3	4.04	3.86	1.47	3.24	3.80
A29	26.5	4.0	52.0	6.67	3.21	1.20	2.70	3.11
A30	26.5	4.5	52.0	5.27	2.40	1.13	3.15	3.58
A31	26.5	5.0	52.0	4.27	3.46	1.39	3.19	3.57
A32	27.9	4.0	54.8	7.02	3.28	1.34	2.76	3.29
A33	27.9	4.5	54.8	5.55	3.12	1.13	3.22	3.59
A34	27.9	5.0	54.8	4.50	3.18	1.21	2.60	3.16
A35	27.9	5.5	54.8	3.72	3.03	1.18	2.94	3.62
A36	27.9	6.0	54.8	3.12	2.79	1.12	2.99	3.37
A37	29.3	4.0	57.5	7.38	2.72	1.30	2.66	3.14
A38	29.3	4.5	57.5	5.83	3.22	1.19	2.55	3.09
A39	29.3	5.0	57.5	4.72	2.93	1.28	3.02	3.52
A40	29.3	5.5	57.5	3.90	3.37	1.13	3.46	4.00

(continued)

A41	30.7	4.0	60.3	7.73	3.50	1.29	2.86	3.27
A42	30.7	4.5	60.3	6.11	3.11	1.18	2.87	3.34
A43	30.7	5.0	60.3	4.95	3.51	1.24	2.73	3.14
A44	30.7	5.5	60.3	4.09	3.79	1.16	3.60	4.03
A45	30.7	6.0	60.3	3.44	3.25	1.18	3.24	3.98
A46	32.1	4.0	63.0	8.08	3.14	1.16	2.71	3.18
A47	32.1	4.5	63.0	6.39	3.69	1.26	2.89	3.16
A48	32.1	5.0	63.0	5.17	2.92	1.20	2.66	3.11
A49	32.1	5.5	63.0	4.27	3.98	1.16	3.29	3.70
A50	32.1	6.0	63.0	3.59	3.22	1.14	2.32	2.95
A51	32.1	6.0	63.0	3.59	3.44	1.10	3.19	3.59
A52	33.5	4.0	65.8	8.43	2.70	1.07	2.22	2.55
A53	33.5	4.5	65.8	6.66	2.97	1.05	2.69	3.06
A54	33.5	5.0	65.8	5.40	3.27	1.12	2.68	3.12
A55	33.5	5.5	65.8	4.46	3.70	1.23	3.25	3.91
A56	33.5	6.0	65.8	3.75	2.92	1.04	2.27	2.78
A57	33.5	6.0	65.8	3.75	3.66	1.08	2.99	3.38
A58	33.5	6.5	65.8	3.19	4.00	1.24	3.01	3.56

Table 3. Force Coefficients for Cylinder B.

Run	A, in centi-meters	T, in seconds	KC number	Acceler-ation of flow, a_m/g	Inertia coeffi-cient, $\bar{C}_M$	Drag coeffi-cient, $\bar{C}_D$	Lift coeffi-cient, $\bar{C}_L$	Significant lift coefficient $\bar{C}_{Lmax}$
B1	2.8	2.0	2.9	2.82×10^{-2}	1.75	3.38	7.94	10.20
B2	4.2	2.0	4.4	4.23	1.80	2.55	6.20	6.77
B3	4.2	3.0	4.4	1.88	2.06	1.76	7.14	10.83
B4	5.6	2.0	5.9	5.64	1.97	2.34	5.72	6.16
B5	5.6	3.0	5.9	2.51	1.95	1.93	7.53	8.76
B6	7.0	3.0	7.3	3.13	1.82	2.10	6.68	7.09
B7	7.0	4.0	7.3	1.76	1.74	2.14	7.61	8.71
B8	10.5	4.0	11.0	2.64	1.79	1.92	6.17	6.60
B9	14.0	5.0	14.7	2.26	1.90	1.72	5.76	6.33
B10	17.5	6.0	18.3	1.96	2.51	1.64	5.22	6.17
B11	20.9	7.0	21.9	1.72	2.67	1.47	4.98	5.73

Table 4. Force Coefficients for Cylinder C.

Run	A, in centi-meters	T, in seconds	KC number	Acceler-ation of flow, a_m/g	Inertia coeffi-cient, $\bar{C}_M$	Drag coeffi-cient, $\bar{C}_D$	Lift coeffi-cient, $\bar{C}_L$	Significant lift coefficient $\bar{C}_{Lmax}$
C1	5.2	3.0	5.4	2.33×10^{-2}	2.10	2.19	7.87	8.66
C2	7.0	3.0	7.3	3.13	1.98	2.00	7.33	8.00
C3	7.0	4.0	7.3	1.76	1.96	1.98	7.97	8.87
C4	8.7	3.0	9.1	3.89	1.87	2.17	5.97	6.52
C5	8.7	4.0	9.1	2.19	1.91	1.94	6.72	7.35

(continued)

C6	10.5	3.0	11.0	4.70	2.02	2.11	5.76	6.37
C7	10.5	4.0	11.0	2.64	1.89	1.67	6.50	7.04
C8	10.5	5.0	11.0	1.69	2.30	1.86	7.50	8.54
C9	12.2	3.0	12.8	5.46	2.15	1.75	5.39	6.03
C10	12.2	4.0	12.8	3.07	2.15	1.85	5.55	6.38
C11	12.2	5.0	12.8	1.97	2.24	1.69	5.82	6.76
C12	14.0	3.0	14.7	6.27	2.26	1.64	5.19	5.71
C13	14.0	4.0	14.7	3.52	2.22	1.55	5.25	5.87
C14	14.0	5.0	14.7	2.26	2.62	1.63	5.89	6.48
C15	14.0	6.0	14.7	1.57	2.49	1.66	6.47	7.63
C16	15.7	3.0	16.4	7.03	2.16	1.74	4.83	5.33
C17	15.7	4.0	16.4	3.95	2.38	1.49	5.09	5.61
C18	15.7	5.0	16.4	2.53	2.45	1.74	5.43	6.29
C19	17.5	3.0	18.3	7.83	2.29	1.68	4.49	4.97
C20	17.5	4.0	18.3	4.41	2.39	1.67	4.81	5.44
C21	17.5	5.0	18.3	2.82	2.72	1.69	5.26	5.76
C22	17.5	6.0	18.3	1.96	2.82	1.40	5.69	6.40
C23	17.5	7.0	18.3	1.44	2.70	1.58	5.04	5.75
C24	17.5	7.0	18.3	1.44	2.75	1.42	5.39	6.28
C25	19.2	3.0	20.1	8.59	2.33	1.62	4.36	4.80
C26	19.2	5.0	20.1	3.09	2.37	1.51	4.58	5.23
C27	19.2	7.0	20.1	1.58	2.89	1.52	4.63	5.61
C28	20.9	3.0	21.9	9.35	2.11	1.56	3.83	4.17
C29	20.9	4.0	21.9	5.26	2.41	1.56	4.19	4.83
C30	20.9	5.0	21.9	3.37	2.58	1.59	4.25	4.76
C31	20.9	6.0	21.9	2.34	2.90	1.51	5.10	5.71
C32	20.9	7.0	21.9	1.72	2.61	1.52	5.38	5.95
C33	20.9	8.0	21.9	1.32	3.14	1.41	5.40	6.44
C34	22.7	3.0	23.8	10.16	2.11	1.42	3.95	4.37
C35	22.7	5.0	23.8	3.66	2.44	1.46	4.28	4.59
C36	22.7	7.0	23.8	1.87	2.87	1.43	4.82	5.66
C37	24.4	4.0	25.6	6.14	2.84	1.40	4.21	4.90
C38	24.4	5.0	25.6	3.93	2.51	1.40	4.21	4.87
C39	24.4	6.0	25.6	2.73	2.75	1.37	4.73	5.48
C40	24.4	7.0	25.6	2.01	2.64	1.39	5.16	5.81
C41	24.4	8.0	25.6	1.54	3.00	1.36	5.14	5.80
C42	24.4	9.0	25.6	1.21	3.04	1.34	5.20	6.38
C43	26.2	5.0	27.4	4.22	2.73	1.34	4.21	4.92
C44	26.2	7.0	27.4	2.15	3.11	1.30	4.69	5.57
C45	26.2	9.0	27.4	1.30	2.94	1.22	4.30	5.07
C46	27.9	4.0	29.2	7.02	2.71	1.37	3.93	4.48
C47	27.9	5.0	29.2	4.50	2.84	1.31	4.03	4.65
C48	27.9	6.0	29.2	3.12	2.96	1.36	4.59	5.17
C49	27.9	7.0	29.2	2.29	3.09	1.28	4.74	5.45
C50	27.9	8.0	29.2	1.76	3.07	1.27	4.79	5.69
C51	27.9	9.0	29.2	1.39	3.22	1.20	4.61	5.45
C52	27.9	10.0	29.2	1.12	3.24	1.22	4.71	5.69
C53	29.7	5.0	31.1	4.79	3.09	1.28	3.92	4.51
C54	29.7	7.0	31.1	2.44	3.34	1.19	4.39	5.22
C55	29.7	9.0	31.1	1.48	3.31	1.19	4.89	5.84
C56	31.4	5.0	32.9	5.06	2.49	1.25	3.68	4.30
C57	31.4	6.0	32.9	3.51	3.03	1.21	3.80	4.46
C58	31.4	7.0	32.9	2.58	3.27	1.17	3.90	4.65
C59	31.4	8.0	32.9	1.98	3.36	1.13	4.45	5.58
C60	31.4	9.0	32.9	1.56	3.15	1.17	3.68	4.29
C61	31.4	10.0	32.9	1.26	3.31	1.15	3.99	4.72
C62	31.4	11.0	32.9	1.05	3.23	1.12	4.14	5.29
C63	33.2	5.0	34.8	5.35	2.76	1.31	3.86	4.55
C64	33.2	7.0	34.8	2.73	3.06	1.26	3.99	4.81
C65	33.2	9.0	34.8	1.65	3.34	1.17	4.38	4.89
C66	33.2	11.0	34.8	1.11	3.51	1.08	4.28	5.10
C67	33.5	5.0	35.1	5.40	3.32	1.30	3.80	4.36

which is significantly different from that of the lift force in oscillatory flow of large extent (see Ref. 1). The lift force directs always upward for circular cylinders laid on the plane boundary (Fig. 4), as observed by Yamamoto et al (8).

The phases at which the lift forces are maximized in a cycle of oscillating flow, θ_{max}, were measured. The results are depicted in Fig. 5 as a function of the KC number, from which it is revealed that they take π and 2π for relatively low KC number, and reach nearly constant values of about $2\pi/3$ and $5\pi/3$ for KC > 10. Thus, the phase θ_{max} is fixed for sufficiently large KC number.

The lift coefficients $\overline{C}_L$ depicted in Fig. 6 show considerable scatters, but they have an apparent trend to decrease monotonously with an increase of the KC number and to reach a constant value of about 3. The lift coefficients are about three times large than the drag coefficients for wide range of the KC number. The coefficients are again grouped very well if they are parameterized by a_m/g. Any coherent correlation cannot be found for the parameter $\sqrt{\nu T}/D$ which was a significant parameter for the lift coefficients of cylinders immersed in the flow of large extent.

The lift coefficients for flows with large extent are known to have several peaks corressponding to the KC numbers for which the vortex shedding is stable in pattern and in number, and the generation of the lift force is mainly due to alternative shedding of vortices (see e.g. Ref. 1). The observations mentioned in the above postulate that the lift force generation for cylinders placed on plane boundary is mainly due to the mean flow field such as undisturbed flow velocity and acceleration, and the vortex plays relatively a minor role in the lift force generation.

The significant lift coefficient $\overline{C}_{Lmax}$ was introduced to know how large lift force would be possible if the KC number and a_m/g are specified. This coefficient is especially important from the practical point of view, because the lift force is much larger than the other forces, and it affects seriously the design of pipes and cables placed on the boundary. The ratios $\overline{C}_{Lmax}/\overline{C}_L$ can be calculated from Tables 2, 3 and 4 for each cylinder, from which it is revealed that the rations rarely exceed 1.2. The ratios frequently reach 1.5 for flows of large extent for which the beat of the lift force is sometimes found due to the unsteadiness of vortex shedding (see Ref. 1).

Thus, the generation of lift force is relatively stable for cylinders laid on the plane boundary, and it also supports the aforementioned postulate that the lift force is mainly produced under the action of mean flow field.

The data on the coefficients are summarized in Table 2, 3 and 4.

APPLICATION OF FLOW VISUALIZATION

If the mean oscillating flow field is the major agency of the lift force, the location of the separation point must seriously influence the force generation. The flow field near cylinders was thus visualized. As aforementioned, the maximum lift force in a cycle of oscillatory flow occurs at about $\theta_{max} = 2\pi/3$ or $5\pi/3$ for sufficiently large KC number. Therefore, the separation points were observed at $\theta_{max} = 2\pi/3$ using 16 mm cinefilms. Fig. 7 is the motion pictures of identical KC number but different period of oscillatory flow (different acceleration), from which it is clearly revealed that the separation point at θ_{max} moves downstream as the period of flow increases, i. e. as the acceleration of flow decreases. The same tendency is seen in Fig. 8 in which the data at different KC numbers are included. As is well known, the separation point is significantly correlated with the acceleration of flow if the turbulence level is identical. This is true also in the present case, and the separation point moves upstream with increase of a_m/g even if KC is identical. This can explain why the lift coefficients are grouped very well as a function of a_m/g in Fig. 6. The same reasoning can be applied to the inertia coefficients, because they are also significantly correlated with the local flow field near cylinders (see e. g. Ref. 3).

(a)

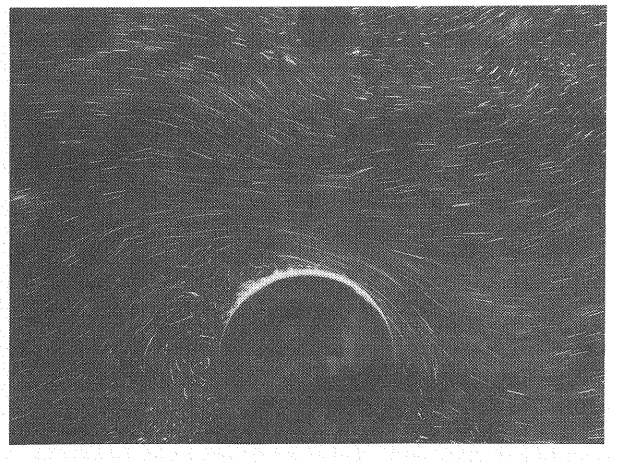

(b)

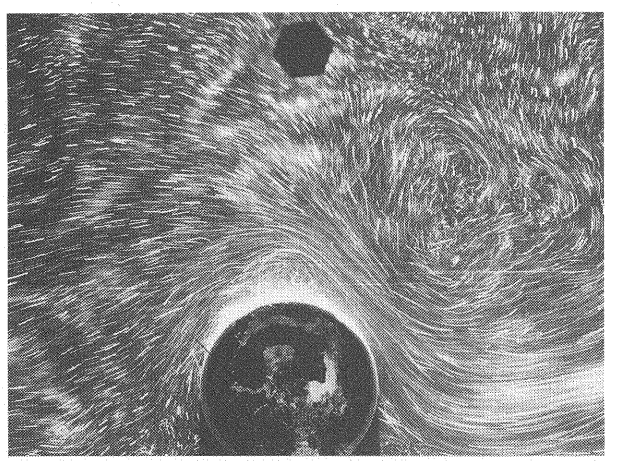

(c)

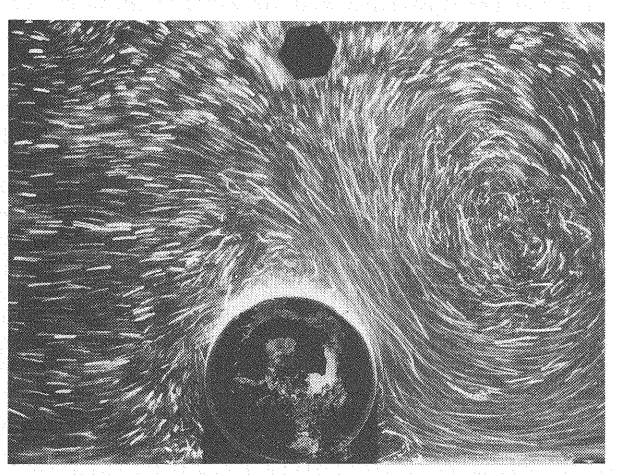

Fig. 7. Flow around Cylinder (Diameter = 6 cm) at the Phase of Maximum Lift Force ($\theta_{max} = 2\pi/3$). (a) KC = 18.3, T = 9 sec; (b) KC = 18.3, T = 6 sec; and (c) KC = 18.3, T = 3 sec. The flows are from right to left.

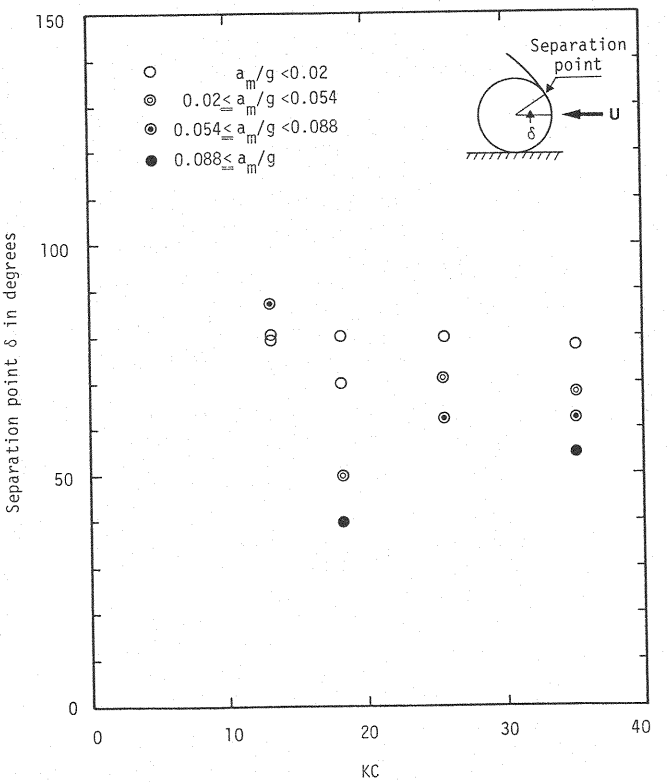

Fig. 8. Separation Point at θ_{max}.

CONCLUSIONS

The inertia, drag and lift forces for circular cylinders placed on the plane boundary are studied in sinusoidally oscillating flows generated in a U-shaped water tunnel. The experiments reveal the followings: (1) The inertia coefficients are well correlated with the KC number and a weak function of the flow acceleration. It takes a value of about 1.8 for low KC number, and it increases monotonously with an increases of the KC number. (2) The drag coefficients show relatively less scatters against the KC number. They decreases as the KC number increases for KC > 7, and they reach a constant value of 1.2. (3) The variation of lift force with time in a period of oscillatory flow has a similar pattern regardless of the KC number if the time scale is normalized by the period of oscillation, and the force generation is fairly stable with respect to time if it is compared with that of cylinders immersed in the oscillatory flow of large extent. The lift coefficients are well correlated with the KC number and are grouped with respect to the acceleration of flow. The lift coefficients are much larger than the drag coefficients. (4) The flow visualization shows clearly how the separation point moves according to the magnitude of acceleration of flow, and which makes clear the reason why the inertia and lift coefficients are grouped as functions of a_m/g.

ACKNOWLEDGMENT

The writers would like to appreciate the assistance of H. Nakamura and Y. Kanno in conducting the experimants. A. Fukita typed the manuscript. This research is partly supported by Kashima Foundation (the subject: Prediction of

Waves around Coastal Structures) for the year 1989.

APPENDIX I. - REFERENCES

1. Ikeda, S., and Yamamoto, Y., : Lift Force on Cylinders in Oscillating Flows, Thechnical Report of Foundation Engineering, Saitama University, Vol.10, 1981, pp.1-16.
2. Keulegan, G.H., and Carpenter, L.H., : Forces on Cylinders and Plates in an Oscillating Fluid, Journal of Research, National Bureau of Standards, Vol.60, 1958, pp.423-440.
3. Milne-Thomson, L.M., : Theoretical Hydrodynamics, 5th ed., The Macmillan Press Ltd., London, England, 1968.
4. Morison, J.R., et al., : The Forces Exerted by Surface Waves on Piles, Petroleum Transactions, American Institute of Mining Engineers, Vol.189, 1950, pp.149-157.
5. Nagasaki, S., and Ogata, K., : Wave Force on Pipe-line Placed on Sea Bottom, Proceedings of 18th Conference on Coastal Engineering, Japan Society of Civil Engineers, 1971, pp.223-227.
6. Sarpkaya, T., : Forces on Cylinders and Spheres in a Sinusoidally Oscillating Fluid, Journal of Applied Mechanics, Transactions of the American Society of Mechanical Engineers, Vol.42, 1975, pp.32-37.
7. Sarpkaya, T., : Forces on Cylinders Near a Plane Boundary in a Sinusoidally Oscillating Fluid, Journal of Fluid Engineering, Transactions of the American Society of Mechanical Engineers, Vol.98, 1976, pp.499-505.
8. Yamamoto, T., Nath, J.H. and Slotta, L.S., : Wave Forces on Cylinders Near Plane Boundary, Journal of the Waterways, Harbors and Coastal Engineering Division, ASCE, Vol.100, No.WW4, 1974, pp.345-360.
9. Wright, J.C., and Yamamoto, T., : Wave Forces on Cylinders Near Plane Boundaries, Journal of the Waterway, Harbor, Coastal and Ocean Division, ASCE, Vol.105, No.WW1, 1979, pp.1-13.

APPENDIX II. - NOTATION

The following symbols are used in this paper:

A = half-amplitude of displacement of undisturbed oscillating flow;
a_m = half-amplitude of acceleration of undisturbed oscillating flow;
C_D = drag coefficient;
C_L = lift coefficient;
C_M = inertia coefficient;
$\overline{C}_D$ = averaged drag coefficient;
$\overline{C}_L$ = averaged lift coefficient;
$\overline{C}_{Lmax}$ = significant lift coefficient;
$\overline{C}_M$ = averaged inertia coefficient;
D = diameter of circular cylinder;
F = force acting on cylinder per unit length;
F_D = drag force acting on cylinder per unit length;
F_M = inertia force acting on cylinder per unit length;
F_X = in-line force acting on cylinder per unit length;
f_n = natural frequency of submerged cylinder;
g = gravitational acceleration;
KC = Keulegan-Carpenter number = U_mT/D;
T = period of oscillatory flow;
t = time;
U = undisturbed oscillatory flow velocity;
U_m = half-amplitude of undisturbed flow velocity;
x = location of undisturbed fluid particle at time t;
δ = angle of separation point from the upstream direction;
θ_{max} = phase at which the lift forces are maximized in a cycle of

oscillatory flow;
μ = viscosity of fluid;
ν = kinematic viscosity of fluid;
ρ = mass density of fluid;
ψ, Ψ, ϕ = functions; and
ω = angular frequency of undisturbed oscillatory flow.